Iraqi Journal of Physics, 2026
https://doi.org/10.30723/ijp.v24i1.1497

Vol.24, No.1, PP.65-75
P-ISSN: 2070-4003
E-ISSN: 2664-5548

Fabrication and Reduction of Graphene Oxide via Hammer Method: Investigation of Structural and Optical Properties

Ahmed. K Sameer[1,2*] and Eman K. Hassan[1]
[1]*Department of Physics, College of Science, University of Baghdad, Baghdad, Iraq*
[2]*Departmentof Physics, College of education for pure Science, University of Anbar, Al-Anbar, Iraq*
[*]Corresponding author: ahmed.k.s1991@uoanbar.edu.iq

Abstract
In this study, reduced graphene oxide (rGO) was synthesized from graphene oxide (GO) via an ascorbic acid-assisted reduction process. GO was synthesized from graphite powder using a modified Hummers technique. The surface morphology, structure, functional groups, and elemental compositions of the produced materials were studied using various methods, such as scanning electron microscopy/energy dispersive X-ray spectroscopy (SEM/EDX), X-ray diffraction (XRD), atomic force microscopy (AFM), Fourier transform infrared (FTIR), and UV-Vis. The removal of oxygen-containing functional groups in rGO through reduction resulted in poor sample quality. In addition, FTIR investigations revealed that GO contained more oxygen-containing functional groups than rGO. Typical peaks at 26.7081° and 26.65° for rGO and GO, respectively, were characterized using XRD. Additionally, a UV-Vis study confirmed the successful reduction by observing a redshift in the absorption peak from 363 nm to 371 nm, indicating partial restoration of the π-conjugation system. Overall, the results demonstrated that graphene oxide was successfully oxidized from graphite and that rGO was efficiently reduced from GO, yielding a material with improved properties for the target application.

Article Info.

Keywords:
Graphene Oxide, Reduction Graphene Oxide, Hummer's Method, XRD, UV-Vis.

Article history:
Received: Jun. 21, 2025
Revised: Oct. 19, 2025
Accepted:Nov. 14, 2025
Published:Mar.01,2026

1. Introduction
Graphene is the most transparent, toughest, thinnest, lightest, and most electrically conductive material in the world [1]. It is a high-density two-dimensional sheet of carbon atoms with a honeycomb-like shape. It has unique properties that make it an interesting material for many industrial applications [2, 3]. Graphite is a crystalline form of carbon. It is a layered structure; the carbon atoms are arranged in hexagonal sheets, where each carbon atom is covalently bonded to three other carbon atoms [4]. Each carbon atom has one non-bonded electron that can move freely along the layers, enabling graphite to conduct electricity. The electrons are subsequently bound by van der Waals forces, which facilitates the separation of the layers. [5]. Modern technologies take into account the versatility of graphite, opening the way for a wide range of reinforcements, including cement. Various reinforcements have significantly contributed to the formation of multi-porous cement, resulting in a highly integrated microstructure [6]. The hybridization of all graphene nano-sheets is sp2, because it contains double bonds at some bonding sites. This makes graphene nano-sheets good conductors due to their zero-energy gap [5]. For this reason, graphene has higher conductivity than all other nano-materials and non-nano-materials, even better than metals, because the carbon on which graphene is based is the lightest and strongest material, and is called super carbon. In addition, graphene has excellent physical, chemical, optical, mechanical, and thermal properties. These properties have made it a widely used material in nano-composite-based industries [7].

Graphene oxide is made up of carbon, oxygen, and hydrogen in various quantities. It can be produced by reacting graphite with strong oxidants and acids. The discovery of graphene oxide is attributed to the German scientist Schafhautt, who observed the

formation of blue graphene when sulfuric acid and nitric acid reacted. Chemist Benjamin Brody was the first to prepare graphene oxide by treating graphene with an oxidizing mixture of nitric acid fumes and potassium chlorate.

Graphene oxide is a single-layer of polycyclic hydrocarbon network with an oxygen and epoxy functional groups. The epoxy and hydroxyl groups are located on the surface of the layer, while the carbonyl and carboxyl groups are located on the edges of the layer [8]. As a result of these groups, graphene oxide sheets are characterized by being hydrophilic. Graphene oxide is easily prepared. However, regardless of the ease of preparation, the oxygen-containing groups are responsible for many of its advantages over graphene, including its high solubility. The presence of these groups on the surface allows it to interact with other compounds physically or chemically and form nano-composites [9]. It is particularly surprising that graphene oxide (GO) can be chemically reduced to graphene-like sheets by removal of oxygen-containing functional groups with retention of conjugated carbon structure. The product obtained, so called Reduced Graphene Oxide (rGO), is generally believed to be a type of chemically-derived graphene. This material is also referred to in the literature as chemically modified graphene, functionalized graphene, chemically converted graphene, or minimized graphene [10]. Although the intrinsic properties of pristine graphene and rGO differ considerably, the fundamental aim of any reduction method is to synthesize graphene-like materials that replicate the mechanical and physical attributes of graphene produced by direct mechanical exfoliation of individual graphite layers.

In this study, the synthesis of GO and rGO was presented, as well as examinations of their morphologies, crystal phases, optical features, quality GO and rGO were examined employing scanning electron microscopy/ Energy Dispersive X-Ray Spectroscopy (SEM/EDX), atomic force microscopy (AFM), Fourier transform infrared (FTIR), and X-ray diffraction (XRD). The improved Hummer method was utilized to synthesize GO, which was then reduced to rGO using ascorbic acid as a minimizing agent.

2. Experimental Part

2.1. Materials

Graphite rod powder (99.995%), sodium nitrate ($NaNO_3$, 99.5%), potassium permanganate ($KMnO_4$) and hydrogen peroxide (H_2O_2) were supplied from Sigma Aldrich, Malaysia. Sulphuric acid (H_2SO_4, 98%) and hydrochloric acid (HCl, 37.5%) were supplied from Chemo Lab, Malaysia. For reducing Graphene oxide, ascorbic acid ($C_6H_8O_6$, 99.8%) (from Merck) was used. Methanol (CH_3OH, 99.8%) was purchased from Fluka.

2.2. Graphene Oxide Synthesis: A Modified Hummer's Process

Graphene oxide was prepared from natural graphite powder employing the Hummer method. In this procedure, 96 ml of concentrated H_2SO_4 was first cooled in an ice bath while being stirred magnetically. Subsequently, 2 g of graphite powder and 1 g of $NaNO_3$ were added to the acid and stirred for one hour. Following this, 4 g of $KMnO_4$ was slowly incorporated into the mixture [11]. Since adding $KMnO_4$ at room temperature poses a risk of explosion, the reaction mixture was maintained below 10 °C using a cold-water bath. $KMnO_4$ was introduced slowly and in small portions to prevent a sudden temperature rise that could occur if it were added all at once. The mixture containing the additional $KMnO_4$ was agitated for 36 hours before being heated for 4 hours at 35 °C. Following that, 500 mL of deionized water was added to the solution, with agitation for an hour.

Finally, 30 wt.% H_2O_2 (5 mL) was added to the diluted solution at room temperature to remove the residual permanganate, and the mixture was allowed to cool for 30 minutes [12]. Then, the product was diluted using approximately 5% hydrochloric acid and water of (HCl (11.25) + H_2O (88.75)), and the distillate was filtered. The graphene oxide precipitate was washed with deionized water several times until a stable pH value of 6 was reached. The separation process was performed using a filtration system. The precipitate was dried in a drying oven at 60 °C for 24 h to remove moisture completely. The final step was washing with ethanol to remove residual impurities. The precipitate was finely ground to obtain a powder. Fig.1 depicts the change of graphite to graphene oxide, whereas Fig. 2 depicts the manufacture of graphene oxide using the improved Hummer process. The chemical reactions describing the probable response of graphite in the presence of sulfuric acid and potassium permanganate are as follows: [11,13]:

(a) Formation of Graphite Intercalation Compound (GIC):

$$C\ (graphite) + H_2SO_4 + NaNO_3 \rightarrow C^{+}HSO^{-}{}_4 \cdot H_2SO_4 \cdot NO_2 + NaOH$$

(b) Oxidation by $KMnO_4$:

$$C^{+}HSO^{-}{}_4 + KMnO_4 \rightarrow \text{Graphene Oxide (GO)} + Mn^{2+} + K^{+} + SO_4^{2-} + H_2O$$

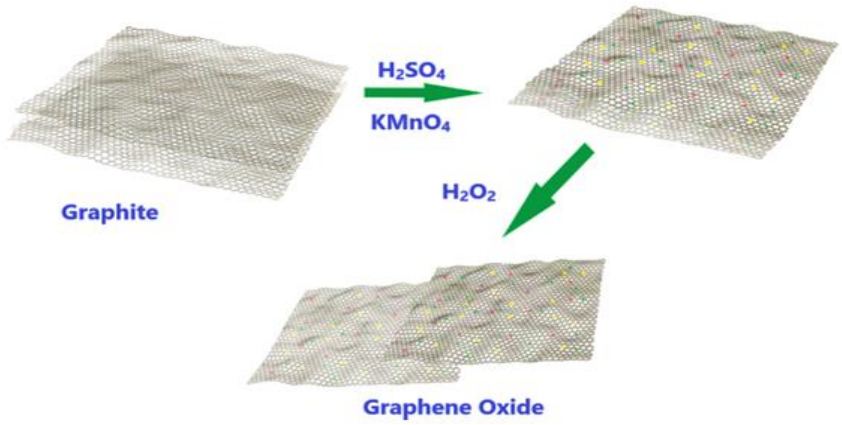

Figure 1: Graphite to Graphene oxide change.

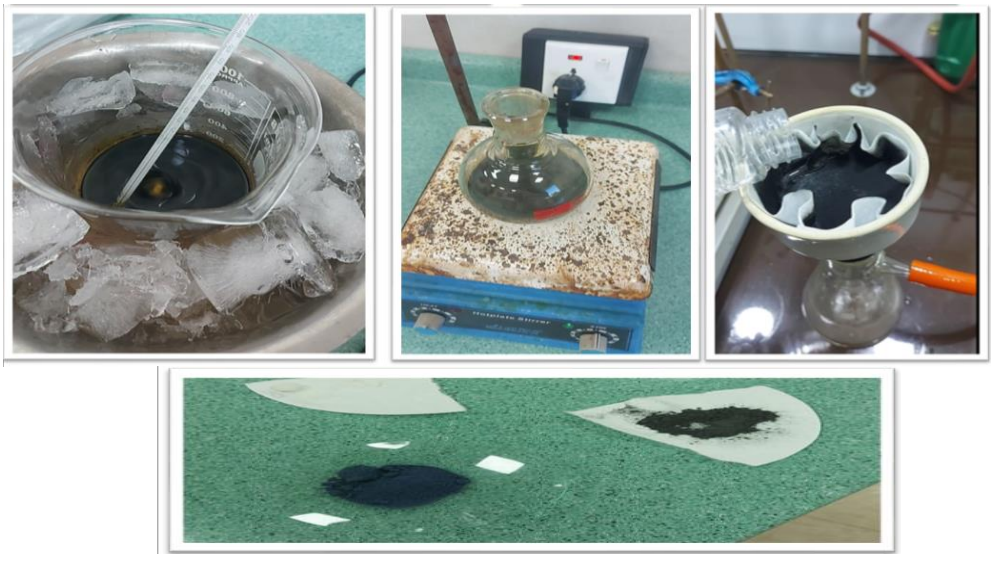

Figure 2: Photos showing graphene oxide synthesis using modified Hummer method.

2.3. Reduction of Graphene Oxide to Reduced Graphene Oxide

9 g of GO powder was mixed with 900 mL of deionized water. Next, 0.9 mL of $C_6H_8O_6$ was added as a minimizing agent for the elimination of oxygen-containing functional groups (e.g., epoxy, hydroxyl, carbonyl, and carboxyl groups) from GO. The mixture was stirred and heated for 90 minutes at 90 °C. The minimized product was obtained using filtration and centrifugation. Finally, the black product was rinsed multiple times with filtered water until the PH reached 6, centrifuged, and dried in an oven at 80°C for 4 hours.

The rGO preparation flow chart and the schematic representation of reduced graphene oxide synthesis are shown in Fig. 3, 4, respectively. The decrease of graphene oxide can be represented as follows [13]:

$$GO\ (Graphene\ Oxide)+C_6H_8O_6 \rightarrow rGO\ (Reduced\ Graphene\ Oxide)+C_6H_6O_6+H_2O$$

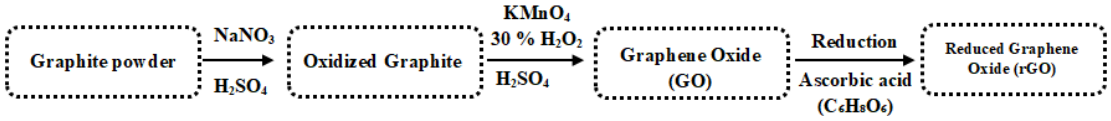

Figure 3: rGO preparation flow chart.

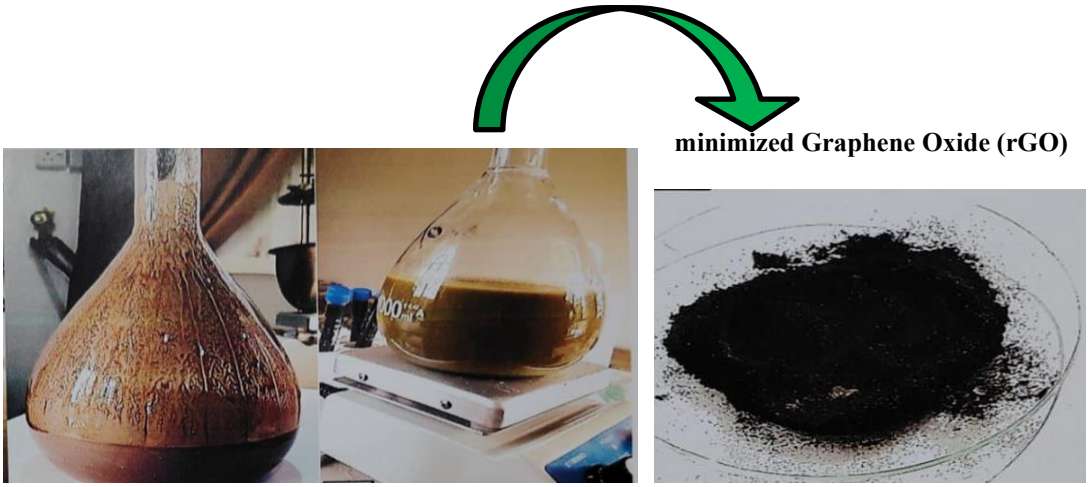

Figure 4: Photos showing the synthesis of reduced graphene oxide.

2.4. Characterization Techniques

A UV-visible spectrometer (PerkinElmer, USA) was used to calculate the absorption spectra of GO and rGO at a wavelength range of 200-900 nm. FTIR (PerkinElmer, USA) was utilized to examine the presence/absence of functional groups on GO and rGO in all samples, within the wavelength range of 4000-400 cm^{-1}. Visual classification entails observing the changes in GO before and after a decrease [14].

EDX (Bruker Nano GmbH, Germany) was employed for the elemental analysis or chemical characterization of a sample [15]. XRD (Shimadzu XRD-6000) examined the crystallinity phase that exist in the samples from 5° to 60° with Cu-Kα radiation (λ=1.5418 Å) to characterize the interlayer spacing. Lastly, for morphological examination, SEM (SEM, Jeol JSM 6460LV) and Atomic Force Microscope (AFM-Angstrom-SPM-AA3000) were used with interaction mode to detect the ultrafine structure (nanostructure) of the thin films with high accuracy exactly of 0.26 nm lateral and 0.1nm vertical) [16].

3. Results and Discussion

3.1. UV-Vis Characterization

To evaluate the oxidation states of GO and rGO, UV-Vis spectroscopy was employed [15,16]. GO and rGO had different characteristics in their spectra, as shown in Fig. 5. For GO, a large absorption peak at 363 nm, attributed to the 2- C-C atomic bonds, corresponding to the 4-3* transitions [12]. Additionally, a shoulder peak near 400 nm was observed, which is associated with n-π* transitions involving the carboxyl (C=O) groups [17] and extensive unoxidized graphite regions. Upon reduction with ascorbic acid, the maximum absorption peak for rGO shifted from 363 to 371 nm, reflecting the substantial removal of oxygen-containing functional groups.

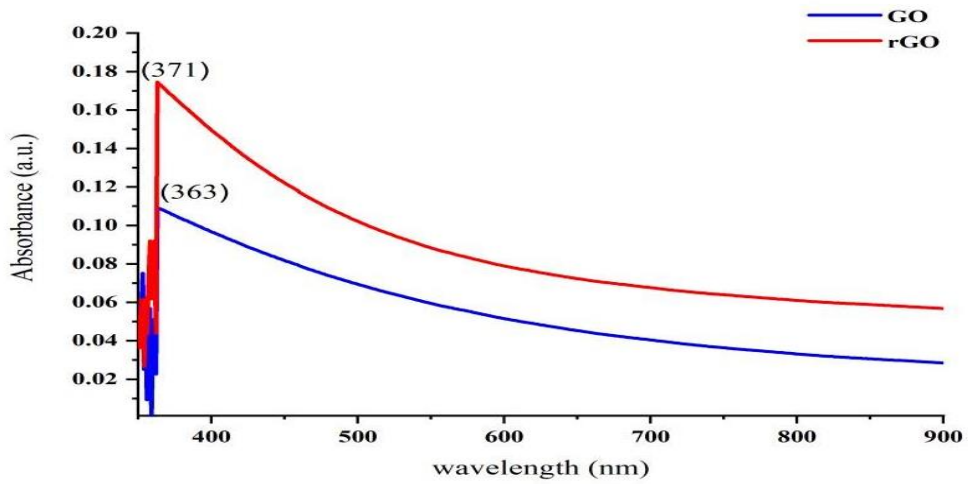

Figure 5: UV-Vis spectra of GO and rGO.

The energy band gap of graphene oxide and reduced graphene oxide was determined using the Tauc plot of $(\alpha h\upsilon)^2$ vs. $h\upsilon$ (Fig. 6). From the plots, the optical band gap of GO was 2 eV, while that of rGO was 1.95 eV. Previous investigations have shown a similar trend for GO, with a larger optical band gap than that of rGO: 2.2 eV for GO and ~1.00 to 1.69 eV for rGO, depending on the degree of reduction using ascorbic acid as the minimizing agent [18]. It is clear that the graphene oxide produced by chemical exfoliation has a higher band gap than the reduced graphene oxide. Therefore, the resulting reduced graphene oxide is used in several applications, including as a humidity sensor.

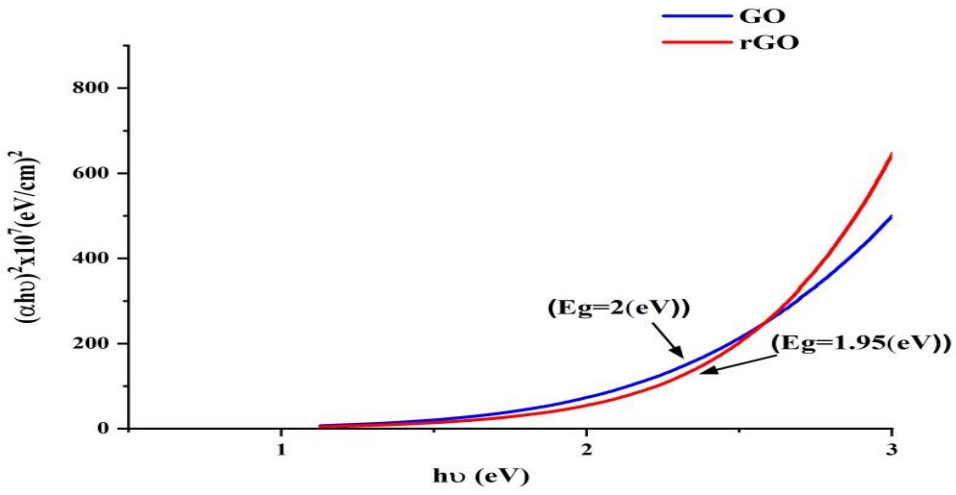

Figure 6: $(\alpha h\upsilon)^2$ vs. $h\upsilon$ for GO and rGO to determine the optical band gap.

3.2 FTIR

Fig. 7 shows the FTIR characterization of GO and rGO. FTIR was performed to identify the functional groups of the studied samples by analyzing the vibrational (transmittance/absorption) spectra. This method of analysis is based on the vibrational excitation of molecular bonding induced by infrared radiation at wavelengths between 4000 and 400 cm^{-1} [19].

As an oxidized form of graphite, GO is known to contain a higher concentration of oxygenated functional groups following its synthesis, whereas rGO is expected to retain only a limited number of such groups after reduction. The FTIR spectra, shown in Fig. 7, reveal several characteristic functional groups, including O–H, C–OH, COOH, and C–O. In GO, a broad peak is observed between 3500 cm^{-1} and 2700 cm^{-1} corresponding to the O–H stretching vibrations of carboxylic acids [20-23]. The absorption peak at 3423 cm^{-1} is attributed to the O–H stretching of adsorbed water molecules and alcohol groups [20]. Besides, increased intensities at 2925 cm^{-1} and 2854 cm^{-1} imply the asymmetric and symmetric stretching vibrations of CH_2 units, respectively [21]. The discrete peak around 1716 cm^{-1} is assigned to the C=O stretching of carboxyl functional groups [24], the 1242 cm^{-1} peak can be attributed to the C–OH stretching variations over alcohol group [22], and the 1037 cm^{-1} peak is related to C-O stretching on C –O- O- C linkages [23].

The rGO spectrum shows significant differences in several peaks compared to the GO peaks, indicating the effectiveness of oxygen functionalization:
OH region (approximately 3423.93 cm^{-1}): This band has a large amplitude, indicating the removal of a significant portion of the hydroxyl groups and, thereby, the successful reduction process. C=C and C-O-C regions: The disappearance or shift of the high-temperature peaks at approximately 1716.63 cm^{-1}, 1242.96 cm^{-1}, and 1037.7565 cm^{-1} indicates the effective removal of carbon and epoxy groups and the restoration of the carbon structure. Appearance of C-H groups: The appearance or clarity of the C-H bond strength peaks is evident at approximately 2925.11 cm^{-1} and 2854.15 cm^{-1}. This may indicate the presence of carbon-hydrogen residues or the rearrangement of some groups at the edge of the rGO layer. This reduction in peak intensity confirms the successful removal of oxygen-containing functional groups from graphene oxide by ascorbic acid treatment, indicating effective conversion to reduced graphene oxide.

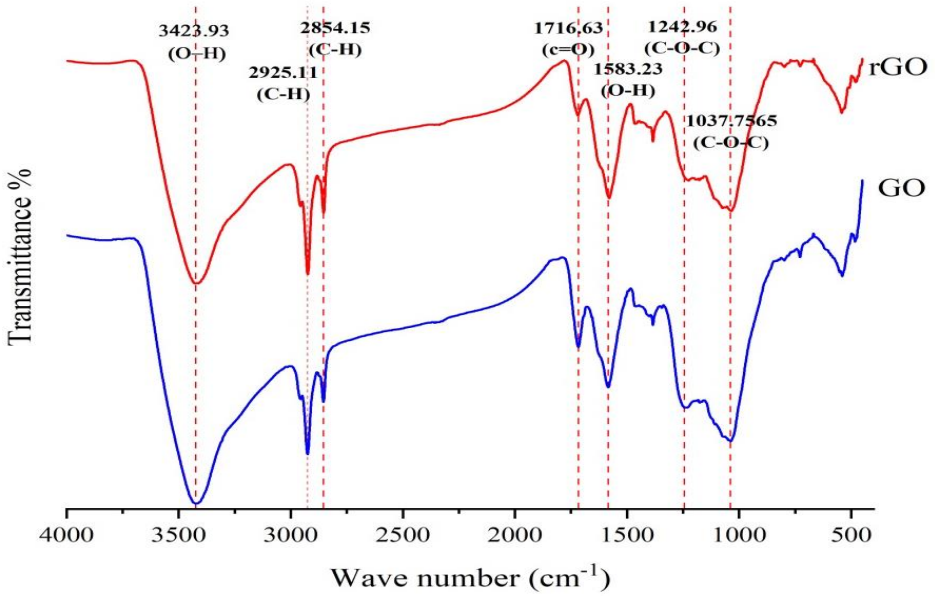

Figure 7: FTIR spectra for GO and rGO.

3.3 EDX and SEM analysis

The surface morphology of GO and rGo was studied using SEM. The SEM images of plane GO and rGO are displayed in Fig. 8 and 9, respectively. EDX of GO in a SEM reveals carbon and oxygen peaks (Fig. 8), along with peaks indicating impurities and reaction residues. Similarly, EDX of rGO shows carbon and oxygen peaks (Fig. 9) but with a reduced oxygen peak intensity compared to GO, reflecting the removal of hydroxyl and carboxyl groups. Minor impurity peaks are also present.

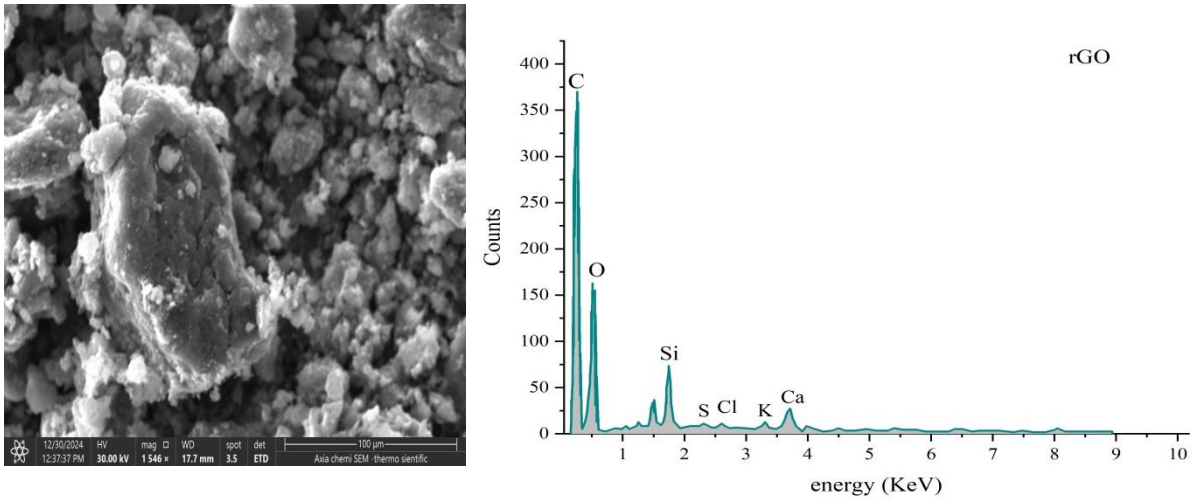

Figure 8: SEM–EDX of Graphene oxide (GO).

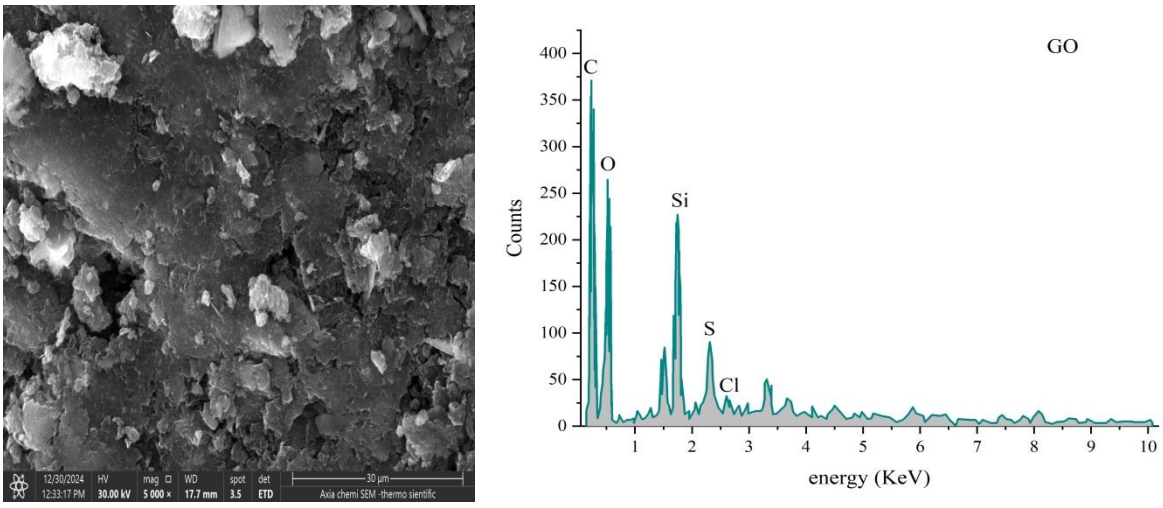

Figure 9: SEM–EDX of minimized Graphene oxide (rGO).

3.4. XRD

To find out the crystalline phases and measure the interlayer spacing of GO and rGO, XRD analysis was carried out. Fig. 10 shows the XRD patterns of the two materials. A highly noticeable peak was observed at $2\theta = 26.65^{o}$, which was attributed to a well-ordered layered structure with a d-spacing of 3.34 A^{o} along the (002) plane [25]. The elimination of the oxygen-based functional groups was also substantial post-reduction, as indicated by the development of a prominent peak at $2\theta = 26.70$ in rGO, which was associated with an interplanar spacing of 3.33 A^{o} along the (002) direction. These results indicate that the p-conjugated structure in graphene was largely recovered in the reduced graphene oxide [26]. The decrease in the interlayer distance occurred because of the disappearance of the oxygenated groups that led to the re-stacking of rGO sheets.

The mean size of crystallites (D) was calculated using the Debye-Scherrer formula in Eq. (1) [27]:

$$D = \frac{k\lambda}{\beta_{hkl} \cos\cos \theta_{hkl}} \quad (1)$$

where k=0.95-0.98 (shape factor), λ = 0.154 nm (X-ray wavelength), β_{hkl}=half-width of the diffraction band (FWHM), θ_{hkl} is the Bragg-diffraction angle (peak position in radians). The crystallite (D) size for graphene oxide was (14.208 nm) and (20.789 nm) for reduced graphene oxide.

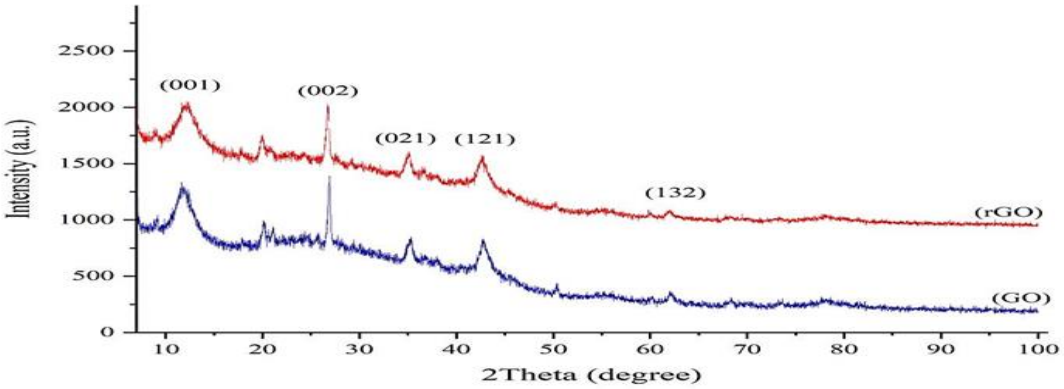

Figure 10: XRD spectra of GO and rGO.

3.5. AFM

AFM revealed the thickness and surface roughness of GO and rGO. AFM images (Fig. 11 and 12) indicated the average thicknesses of 25.84 nm for GO and 21.37 nm for rGO. The graphene oxide surface, characterized by oxygen-containing functional groups, exhibits higher hydrophilicity and dispersibility. As seen in Table 1, rGO demonstrated lower surface roughness than GO; the root mean square (RMS) roughness was 1.73 nm for rGO and 40.37 nm for GO [28]. GO roughness varied with preparation method and the presence of other materials.

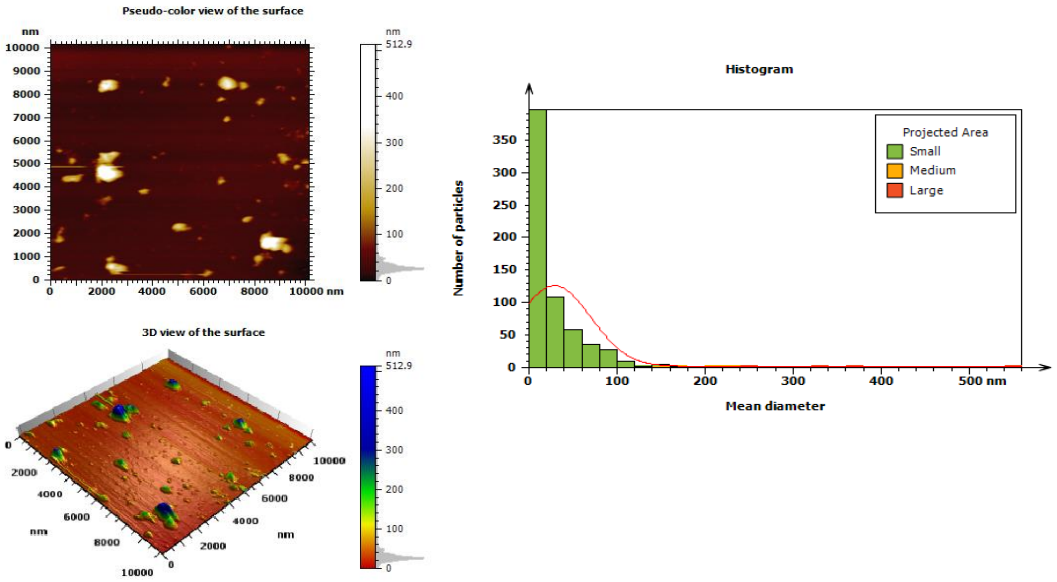

Figure 11: AFM of Graphene oxide.

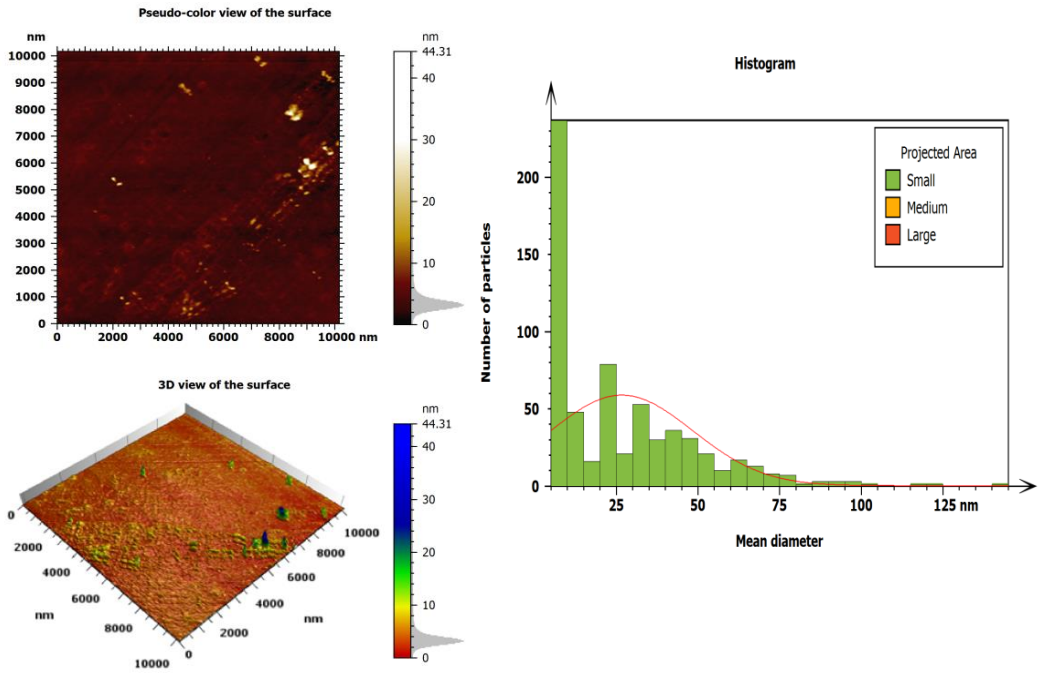

Figure 12: AFM of reduced Graphene oxide.

Table 1: AFM test parameters for GO and rGO.

	Roughness Mean (nm)	Root mean square (nm)	Avg. Diameter (nm)
GO	17.96	40.37	25.847
rGO	0.897	1.731	21.372

4. Conclusions

GO was synthesized via an improved Hummer's method using $KMnO_4$ and H_2SO_4, and subsequently reduced to rGO with ascorbic acid. XRD, SEM, and FTIR analyses confirmed the successful synthesis of both materials. SEM images showed morphological differences between GO and rGO. Furthermore, FTIR tests showed that there was a considerable decrease in the number of oxygenated functional groups in rGO than those present in GO. XRD characterization also revealed their distinctive diffraction peaks; GO exhibited a peak of 26.65º; rGO exhibited a peak of 26.7081º. An energy-dispersive X-ray (EDX) further confirmed the presence of less oxygen in rGO, confirming the elimination of the hydroxyl and carboxyl groups, but small traces were still detected. The energy band gaps, determined from the Tauc plots, were 2 eV for GO and 1.95 eV for rGO, in line with the degradation of oxygen functionalities. Such exceptional physicochemical characteristics of these two forms of GO and rGO indicate that they may be applicable in a vast variety of technological activities.

Conflict of interest

Authors declare that they have no conflict of interest.

References

1. K. M. Janavika, and R. P. Thangaraj, Materialstoday: *Proceedings of 2nd international conference on management and Recycling of metallurgical wastes (metwaste 2023),* edited by K.Singh and A. Meshram,**112**,2024. https://doi.org/10.1016/j.matpr.2023.05.446.
2. M. Rasheed, S. Shihab, and O. W. Sabah, in *2nd International Conference on Materials, Laser science and Applied physics (ICMLAP) 2020*, **1795**, 012052 (2021). https://doi.org/10.1088/1742-6596/1795/1/012052.
3. T. Yusaf, A. S. F. Mahamude, K. Farhana, W. S. W. Harun, K. Kadirgama, D. Ramasamy, M. K. Kamarulzaman, S. Subramonian, S. Hall and H. A. Dhahad, *Sustainability* **14**, 12336 (2022). https://doi.org/10.3390/su141912336.
4. A. Lahbib, B. Lahcen, Y. Khalid, E. Abderrahim, E. A. Abdelmalik, and R. Zahra, Cryst. Struct. Theor. Appl. **12**, 1 (2024). https://doi.org/10.4236/csta.2024.121001.
5. S. Drewniak, T. Pustelny, R. Muzyka, A. Stolarczyk, and G. Konieczny, Photon. Lett. Pol. **7**, 47 (2015). http://www.photonics.pl/PLP/index.php/letters/article/view/7-17.
6. S. H. Haji, F. A. Kochary, and S. M. Ahmed, Sci. J. Univ. Zakho **12**, 14 (2024). https://doi.org/10.25271/sjuoz.2024.12.1.1198.
7. A. A. Musa, A. Bello, S. M. Adams, A. P. Onwualu, V. C. Anye, K. A. Bello, and I. I. Obianyo, Polymers **17**, 893 (2025). https://doi.org/10.3390/polym17070893.
8. H. A. Hessain and J. J. Hassan, Iraqi J. Sci. **61**, 1313 (2020). https://doi.org/10.24996/ijs.2020.61.6.9.
9. S. Qamar, N. Ramzan, and W. Aleem, Synth. Met. **307**, 117697 (2024). https://doi.org/10.1016/j.synthmet.2024.117697.
10. E. Adotey, A. Kurbanova, A. Ospanova, A. Ardakkyzy, Z. Toktarbay, N. Kydyrbay, and O. Toktarbaiuly, Nanomaterials **15**, 363 (2025). https://doi.org/10.3390/nano15050363.
11. N. Sharma, M. Arif, S. Monga, M. Shkir, Y. K. Mishra, and A. Singh, Appl. Surf. Sci. **513**, 145396 (2020). https://doi.org/10.1016/j.apsusc.2020.145396.
12. M. R. Magro, D. A. Vella, and G. Cassar, Cartogr. Remote Sens. **20**, 100509 (2025). https://doi.org/10.1016/j.cartre.2025.100509.
13. P. Kumari, A. Kumar, A. Yadav, Y. Sabri, S. J. Ippolito, D. D. Shivagan, and K. Bapna, Phys. Chem. Chem. Phys. **27**, 3420 (2025). https://doi.org/10.1039/D4CP04347B.
14. H. Aldosari, Nano Hybrids Compos. **37**, 59 (2022). https://doi.org/10.4028/p-72519w.
15. K. Lingaraju, H. R. Naika, G. Nagaraju, and H. Nagabhushana, Biotechnol. Rep. **24**, e00376 (2019). https://doi.org/10.1016/j.btre.2019.e00376
16. N. Naeema, A. Kudher, and G. H. Mohammed, IOP Conf. Ser.: Mater. Sci. Eng. **757**, 012024 (2020). https://iopscience.iop.org/article/10.1088/1757-899X/757/1/012024/meta.
17. N. E. Zikalala, S. Azizi, L. S. Mpeta, R. Ahmed, A. Dube, N. Mketo, A. A. Zinatizadeh, T. Mokrani, and M. M. Maaza, Diamond Relat. Mater. **149**, 111560 (2024). https://doi.org/10.1016/j.diamond.2024.111560.
18. K. M. Katubi, A. Jabeen, Z. A. Alrowaili, I. Shakir, M. S. Al-Buriahi, and M. F. Warsi, Desalin. Water Treat. **322**, 101115 (2025). https://doi.org/10.1016/j.dwt.2025.101115.
19. D. Prodan, M. Moldovan, G. Furtos, C. Saroși, M. Filip, I. Perhaița, R. Carpa, M. Popa, S. Cuc, S. Varvara, and D. Popa, Appl. Sci. **11**, 11330 (2021). https://doi.org/10.3390/app112311330.
20. Z. Mo, Y. Sun, H. Chen, P. Zhang, D. Zuo, Y. Liu, and H. Li, Polymer **46**, 12670 (2005). http://dx.doi.org/10.1016/j.polymer.2005.10.117
21. H. L. Guo, X. F. Wang, Q. Y. Qian, F. B. Wang, and X. H. Xia, ACS Nano **3**, 2653 (2009). https://doi.org/10.1021/nn900227d.
22. T. Y. Zhang and D. Zhang, Bull. Mater. Sci. **34**, 25 (2011). http://dx.doi.org/10.1007/s12034-011-0048-x.
23. Z. Liu and X. Zhou, *Graphene-Based Materials: Synthesis and Applications*, (CRC Press, USA, 2014) 1st edition. https://doi.org/10.1201/b17757
24. L. Shahriary and A. A. Athawale, Int. J. Renew. Energy Environ. Eng. **2**, 58 (2014). https://doi.org/10.1177/0003702818798405 .
25. S. Fazil, K. Liaqat, W. Rehman, S. F. Alam, L. Rasheed, A. Maalik, and M. M. Alanazi, Preprints (2024). https://doi.org/10.20944/preprints202405.1543.v1.

26. O. G. Hammoodi, E. T. B. Al-Tikrity, and K. H. Hassan, World J. Environ. Biosci. **8**, 46 (2019).
27. A. Monshi, M. R. Foroughi, and M. R. Monshi, World J. Nano Sci. Eng. **2**, 154 (2012). http://dx.doi.org/10.4236/wjnse.2012.23020.
28. P. K. Jha, W. Khongnakorn, C. Chawenjkigwanich, M. S. Chowdhury, and K. Techato, Separations **8**, 68 (2021). http://dx.doi.org/10.3390/separations9050129.

تصنيع واختزال أكسيد الجرافين باستخدام طريقة همر: دراسة الخصائص التركيبية والبصرية

احمد كريم سمير[1،2] و ايمان كريم حسن[1]
[1] قسم الفيزياء، كلية العلوم، جامعة بغداد، بغداد، العراق
[2] قسم الفيزياء، كلية العلوم، جامعة الانبار، الانبار، العراق

الخلاصة
في هذه الدراسة، تم تصنيع أكسيد الجرافين المختزل (rGO) من أكسيد الجرافين (GO) عبر عملية اختزال بمساعدة حمض الأسكوربيك. تم تصنيع GO من مسحوق الجرافيت باستخدام تقنية هامر المعدلة. تم التحقيق في مورفولوجيا السطح والبنية والمجموعة الوظيفية وتركيبات العناصر للمواد المنتجة باستخدام طرق مختلفة مثل المجهر الإلكتروني الماسح / مطيافية الأشعة السينية المشتتة للطاقة (SEM/EDX)، حيود الأشعة السينية (XRD)، مجهر القوة الذرية (AFM)، تحويل فورييه بالأشعة تحت الحمراء (FTIR)، والأشعة فوق البنفسجية المرئية (UV-Vis). أدى التخلص من المجموعة الوظيفية المحتوية على الأكسجين من خلال الاختزال لـ rGO إلى تقليل جودة العينة لأن النطاق D كان أكثر كثافة من النطاق G في بيانات رامان. بالإضافة إلى ذلك، كشف بحث تحويل فورييه بالأشعة تحت الحمراء (FTIR) أن GO يحتوي على مجموعات وظيفية تحتوي على الأكسجين أكثر من rGO. يمكن التعرف على القمم النموذجية عند 26.7081 درجة و26.65 درجة لـ rGO وGO، على التوالي، باستخدام الأشعة السينية للحيود. بالإضافة إلى ذلك، أدى الانخفاض إلى انزياح أحمر عند طول موجي 371 نانومتر من 363 نانومتر، كما حُدد من خلال فحص الأشعة فوق البنفسجية المرئية (UV-Vis). أظهرت النتائج أن أكسيد الجرافين (GO) يتأكسد بفعالية من الجرافيت، بينما يُختزل أكسيد الجرافين (rGO) بفعالية من أكسيد الجرافين.

الكلمات المفتاحيه: أكسيد الجرافين، اختزال أكسيد الجرافين، طريقة هامر، حيود الأشعة السينية، الاشعة فوق البنفسجية.